

PH4052D Project Part II

Report

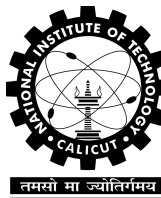
**Study of Single Scattering Albedo of Microplastic
Aerosols using Incoherent Broadband Cavity
Enhanced Absorption Spectroscopy and
Aethalometer**

*Submitted in partial fulfilment of
the requirements for the award of the degree of*

**Bachelor of Technology
in
Engineering Physics**

Submitted by
Reuben S Mathew B200150EP

Under the guidance of
Dr. M K Ravi Varma



Department of Physics
NATIONAL INSTITUTE OF TECHNOLOGY CALICUT
Calicut, Kerala, India – 673 601
Winter Semester 2023-24

Declaration

I declare that this report, titled "**Study of Single Scattering Albedo of Microplastic Aerosols using Incoherent Broadband Cavity Enhanced Absorption Spectroscopy and Aethalometer**" submitted in partial fulfilment of the degree of **B. Tech in Engineering Physics** is a record of original work carried out by me under the supervision of **Dr M K Ravi Varma**, and has not formed the basis for the award of any other degree or diploma, in this or any other Institution or University. In keeping with the ethical practice of reporting scientific information, due acknowledgements have been made where the findings of others have been cited.

Reuben S Mathew

B200150EP

National Institute of Technology, Calicut

30 April 2024

Certificate

This is to certify that this report, titled "**Study of Single Scattering Albedo of Microplastic Aerosols using Incoherent Broadband Cavity Enhanced Absorption Spectroscopy and Aethalometer**" is a bona fide record of the project done by Reuben S Mathew (*Roll no. B200150EP*) under my supervision, in partial fulfilment of the requirements for the award of the degree of **Bachelor of Technology in Engineering Physics** from **National Institute of Technology, Calicut**, and this work has not been submitted elsewhere for the award of the degree.

Dr. M K Ravi Varma

(Project Guide)

Dept. of Physics

Head

Dept. of Physics

Place: National Institute of Technology, Calicut

Date: 30 April 2024

Acknowledgements

I would like to express my sincere gratitude to my guide, Prof. M K Ravi Varma, for his invaluable guidance, unwavering support, and profound insights throughout the course of this research. His expertise and encouragement have been instrumental in shaping the direction and quality of this work.

I would also like to extend my appreciation to Salma Jose. Her unwavering support, patient guidance and valuable insights has played a pivotal role in the success of this project to its fullest potential.

I am deeply thankful for the support of the other dedicated faculty members at the Department of Physics, National Institute of Technology, Calicut. Their collective wisdom and encouragement have been instrumental in my academic journey. Special thanks to Prof. Sujith A, Department of Chemistry for his advice and support at various points over the course of the project.

My heartfelt thanks also go out to my family and friends for their unwavering support and for lending a helping hand when needed. Their encouragement has been a source of strength, and I am truly grateful for their presence in my life.

April 2023

National Institute of Technology Calicut

Abstract

Plastics are quintessential to everyday life. They are present in most everyday items, and their use is increasing at an exponential rate [1]. During use and after disposal they weather and break down into smaller fragments, and proliferate into various ecosystems. Studies are ongoing to determine the effects of microplastic on the ecosystem and human health. Another important effect to consider is the impact of microplastic aerosols on the Earth's climate. They can scatter or absorb light and lead to substantial warming or cooling of the climate. Computer models have been made to investigate such effects [2], but actual experimental data is lacking.

This report goes over a method to study the single scattering albedo of microplastic aerosols using a combination of highly sensitive cavity enhanced absorption spectroscopy and an aethalometer, and proves the feasibility of real-time in-situ measurements of single scattering albedos of microplastic aerosols to study it's radiative forcing effects.

Contents

List of Figures	iv
1 Introduction	1
1.1 Background and Motivation	1
1.2 Microplastics	2
1.3 Single Scattering Albedo	3
2 Instruments	5
2.1 Incoherent Broadband Cavity Enhanced Absorption Spectroscopy (IB-BCEAS)	5
2.2 Aethalometer	8
3 Experimental Setup	10
3.1 Creating microplastic solution	11
3.2 Generation of aerosols	11
3.3 Sample Dryer	12
3.4 $2.5\mu\text{m}$ filter	13
3.5 Light sources	13
3.6 400 to 550 nm Cavity	14
3.7 650 to 680 nm Cavity	14
3.8 Aethalometer	14
3.9 Connections and Source	15
4 Building and Calibrating the IBBCEAS Cavities	16
4.1 Cavity setup	16
4.1.1 Initial setup and laser alignment	16

4.1.2	Arc lamp alignment	16
4.1.3	HR mirror alignment	17
4.1.4	Output light collection	17
4.1.5	Verification and optimization	17
4.1.6	Chamber mounting	18
4.2	Cavity Calibration	18
5	Experiments and data collection:	20
5.1	Data collection	20
5.2	Data analysis and results	21
6	Discussions and outlook	23

List of Figures

1.1	Common sources of plastic waste and debris	2
1.2	Various sources of atmospheric microplastics,[9]	3
2.1	IBBCEAS cavity	6
2.2	Magee Scientific AE33 Aethalometer	8
3.1	Schematic of the entire measurement setup	10
3.3	Magee Scientific sample air drier	13
3.6	Lab setup	15
4.2	Reflectivity spectrum of both cavities	19
5.1	Data collected from the various instruments	20
5.2	Absorption coefficient with power law fitting	21
5.3	Extinction spectrum, with power law fitting	22
5.4	Single Scattering Albedo	22

Chapter 1

Introduction

1.1 Background and Motivation

Proper characterisation of the radiative forcing effects of microplastic aerosols are paramount to understanding the extent of its effect on the climate. Many techniques have been proposed to help identify and characterise the chemical composition and physical properties of microplastics[3]. Modelling studies done conclude that the radiative forcing effects of microplastics are substantial, but still negligible compared to the effects of other aerosols, but experimental study of its effect on climate is lacking[2]. Plastic waste is growing, and owing to its durability, the concentration is unlikely to come down naturally. Definitive experimental research on the climate effects is crucial to support legislation and improve public awareness of yet another harmful effect of plastic waste.

Single Scattering Albedo (SSA) is a crucial factor in determining radiative forcing. Radiative forcing is a measure of how variation in concentration of climate-change drivers in the atmosphere affects the net energy radiated from the troposphere. Comprehensive study of the Single scattering albedo of aerosol microplastics can provide more insights into their contribution to global warming/cooling.

This report encapsulates the work done to develop an experimental setup to study the Single scattering albedo of microplastics aerosols. Single scattering albedo can be determined by studying any two of the absorption, scattering or extinction coefficient of the aerosol [4]. Two highly sensitive Incoherent Broadband Absorption Cavity Enhanced Spectroscopy (IBBCEAS) setups, working over 400 to 550 nm and 650 to

680 nm wavelength ranges were used to study extinction coefficient over a large range of the visible spectrum. An off the shelf aethalometer is used to obtain their absorption coefficients.

This report briefs the various components used, data collection methods, analysis and discusses the results obtained.

1.2 Microplastics

Microplastics are formally defined as plastic debris of size less than [5]. They are a global environmental pollutant which are of increasing concern. The robustness of plastics has led to a rise in generation and poor disposal of waste has lead to large sources of plastics. Over time, they break down or wear into smaller microplastics and have been recently discovered in various ecosystems across land and sea [6]. They persist in the environment and do not biodegrade. Limited data from animal studies have shown that airborne microplastics can accumulate and cause particle toxicity and induce an immune response but the full extent of its harmful effect on the ecosystem and climate is still under study.

Of particular concern is the rapid rise of airborne microplastics. They originate mainly from industrial emissions, burning of plastic waste and from marine sources. They have been found in animal lungs and also have the potential to affect the Earth's climate through its radiative forcing effects [7, 2]. The extent of the harmful effects of microplastics to both the ecosystem and climate is still unknown.

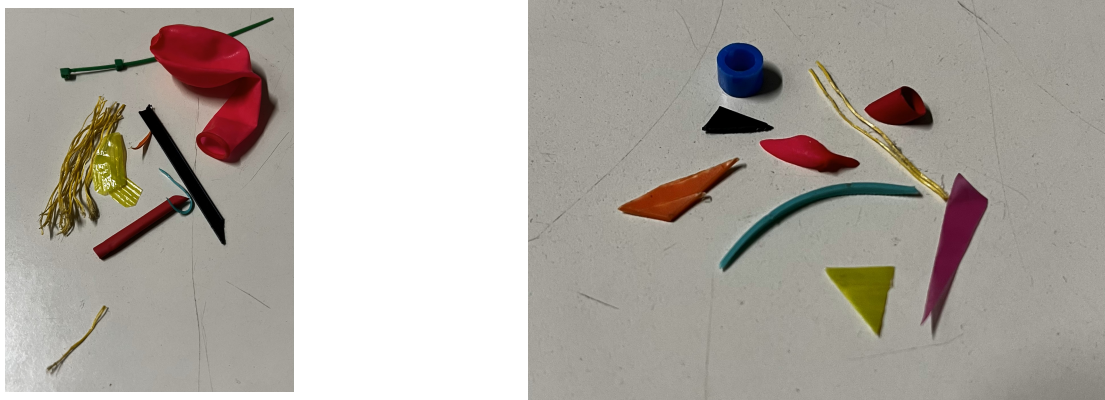


Figure 1.1: Common sources of plastic waste and debris

Although various analytical methods for characterization for microplastics like

SEM, Raman Spectroscopy, Laser Diffraction size analysis and chemical analysis methods have been proposed[3], proper identification and characterization standards for microplastics do not exist [8].

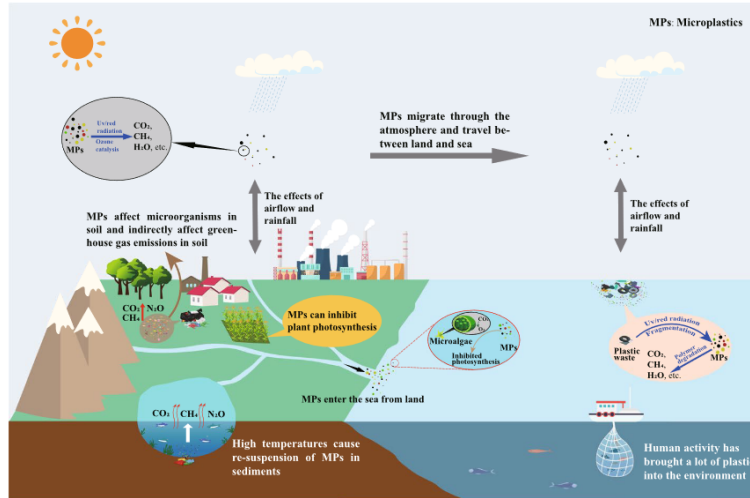


Figure 1.2: Various sources of atmospheric microplastics,[9]

1.3 Single Scattering Albedo

Single Scattering Albedo (SSA) of a given medium is the ratio of scattering coefficient to extinction coefficient. In other terms, it is the fraction of intensity loss attributed only to scattering[10]. This parameter is used to determine both the sign and magnitude of aerosol radiative forcing.

Scattering aerosols have higher SSA values (0.5 - 1), and absorbing aerosols have lower SSA values (0.1 - 0.5). White aerosols predominantly scatter and generally have higher SSA values, leading to a cooling effect on the climate. These aerosols scatter a part of incoming solar radiation back into space, reducing the amount of sunlight intensity reaching Earth's surface. The magnitude of this cooling effect depends on aerosol size, concentration, composition and characteristics of the aerosol surface[11]

The extinction coefficient $\epsilon(\lambda)$ of a medium determines how much light intensity is absorbed when it passes through a material. When a light beam of intensity $I(x)$ passes dx distance through a medium, it will absorb a fraction of the intensity as:

$$\frac{dI}{dx} = -\epsilon dx \quad (1.1)$$

which gives,

$$I(x) = I_0 e^{-\epsilon x} \quad (1.2)$$

The absorption coefficient represents the loss of light intensity due to only absorption, ignoring scattering losses.

Chapter 2

Instruments

2.1 Incoherent Broadband Cavity Enhanced Absorption Spectroscopy (IBBCEAS)

An Incoherent Broadband Cavity Enhanced Absorption Spectrometer (IBBCEAS) measures the attenuation of light transmitted through a high finesse optical cavity to calculate the extinction coefficient of aerosols. It utilises a broadband light source like an arc lamp so that measurements can be made across a large spectrum to simultaneously detect the effects of multiple components[12].

An IBBCEAS setup consists of two high reflecting mirrors ($\sim 99.9\%$) forming a cavity resonator. As shown in Fig. 2.1, light incidents from the left side, with only less than .1% of intensity entering cavity. It passes through the medium, which attenuates the intensity, and hits the other mirror where a fraction of the incident intensity comes out, and the rest is sent back into the cavity and hits the first mirror, further attenuated by the material. This cycle repeats, each pass integrated with the rest and enhancing the attenuative effects of the medium inside the cavity [13].

The intensity of light exiting the cavity after the first pass if given by [13]:

$$I_0 = I_{in}(1 - R)(1 - L)(1 - R) \quad (2.1)$$

The remaining light is reflected back into the cavity, which after reflecting on both the mirrors exit the cavity again. The intensity is given by:

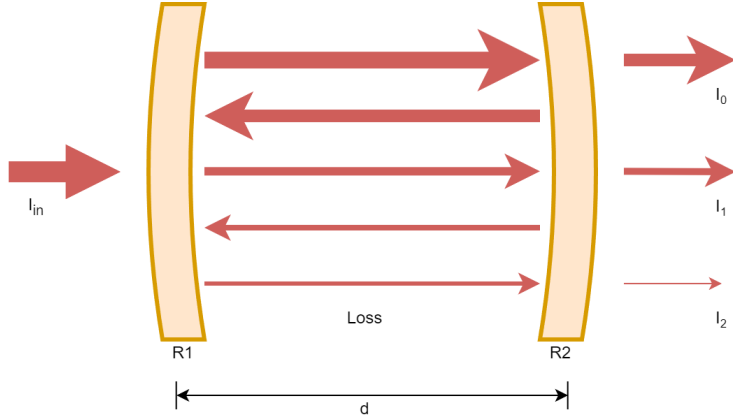


Figure 2.1: IBBCEAS cavity

$$I_1 = I_{in}(1 - R)(1 - L)(R)(1 - L)(R)(1 - L)(1 - R) = I_{in}(1 - R)^2(1 - L)^3R^2 \quad (2.2)$$

This process repeats, and for the n^{th} pass:

$$I_n = I_{in}(1 - R)^2(1 - L)(1 - L)^{2n}R^{2n} \quad (2.3)$$

The net intensity of light exiting the cavity is the sum of the intensities from all passes:

$$I_{out} = I_0 + I_1 + \dots + I_n = I_{in}(1 - R)^2(1 - L) \sum_0^n (1 - L)^{2n}R^{2n} \quad (2.4)$$

As $R < 1$ and $L < 1$, this geometric progression series will converge to form:

$$I = I_{in} \frac{(1 - R)^2(1 - L)}{1 - R^2(1 - L)^2} \quad (2.5)$$

we also see that:

$$I_O = I_{in} \frac{(1 - R)^2}{1 - R^2} = I_{in} \frac{(1 - R)}{1 + R} \quad (2.6)$$

where I_O is the output intensity for an empty cavity ($L = 0$).

From Lambert-Beer extinction law, the fractional intensity exiting cavity can be related to extinction coefficient as:

$$\frac{I_{out}}{I_{in}} = (1 - L) = e^{-\epsilon d} = k \quad (2.7)$$

from Eq. 2.5 and Eq. 2.6, we get:

$$I = I_{in} \frac{(1-R)^2(1-L)}{1-R^2(1-L)^2} = I_O \frac{(1+R)}{1-R} x \frac{(1-R)^2 k}{1-R^2 k^2} \quad (2.8)$$

rearranging in terms of k :

$$k^2 + \frac{1-R^2}{R^2} \frac{I_O}{I} k - \frac{1}{R^2} = 0 \quad (2.9)$$

solving quadratic:

$$k = \frac{-\frac{1-R^2}{R^2} \frac{I_O}{I} \pm \sqrt{\left(\frac{1-R^2}{R^2} \frac{I_O}{I}\right)^2 + \frac{4}{R^2}}}{2} = e^{-\epsilon d} \quad (2.10)$$

$$\epsilon = \frac{1}{d} \ln \left\{ \sqrt{\left(\frac{1-R^2}{2R^2} \frac{I_O}{I}\right)^2 + \frac{1}{R^2}} - \frac{1-R^2}{2R^2} \frac{I_O}{I} \right\} \quad (2.11)$$

for high reflectivity mirrors, $R \rightarrow 1$, the first term under the root can be neglected, and extinction coefficient approximated as:

$$\epsilon \approx \frac{1}{d} \ln \left\{ \frac{R^2 - 1}{2R^2} \frac{I_O}{I} + \frac{1}{R} \right\} \quad (2.12)$$

$$\approx \frac{1}{d} \ln \left\{ \frac{1}{R} \left(\frac{R^2 - 1}{2R} \frac{I_O}{I} + 1 \right) \right\} \quad (2.13)$$

$$\approx \frac{1}{d} \left[-\ln R + \ln \left\{ \frac{R^2 - 1}{2R} + 1 \right\} \right] \quad (2.14)$$

$$\approx \frac{1}{d} \left[-\ln \{1 - (1-R)\} + \ln \left\{ \frac{R^2 - 1}{2R} + 1 \right\} \right] \quad (2.15)$$

$x \rightarrow 0, \ln(1-x) \sim -x$:

$$\epsilon \approx \frac{1}{d} \left[-(1-R) + \frac{R^2 - 1}{2R} \frac{I_O}{I} \right] \quad (2.16)$$

$$\approx \frac{1}{d} \left[(1-R) \left(-1 + \frac{(1+R)}{2R} \frac{I_O}{I} \right) \right] \quad (2.17)$$

$R \rightarrow 1, (1+R) \sim 2R$

giving, extinction coefficient:

$$\epsilon = \left(\frac{I_O}{I} - 1 \right) \frac{(1 - R)}{d} \quad (2.18)$$

2.2 Aethalometer

An aethalometer measures the concentration of black carbon; soot or airborne particulates in the atmosphere. A stream of gas containing the aerosol is passed through a filter, trapping the particulates. A light beam is shined onto the deposited patch and the absorptive attenuation of the patch is calculated. The machine makes periodic measurements to give real time readings of the Black Carbon (BC) concentration of the gas stream.

An AE33 aethalometer by Magee Scientific was used for this project. The absorption coefficient can be derived from “standard black carbon concentration” readout by multiplying it with the absorption coefficient of air, as per the formula [14].

$$\alpha(\lambda) = BC_\lambda * \sigma_{air}(\lambda) \quad (2.19)$$

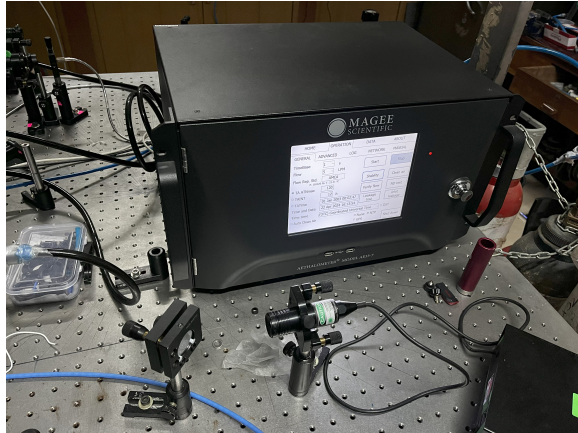


Figure 2.2: Magee Scientific AE33 Aethalometer

The aethalometer can also be used to find the Angstrom exponent (γ). The dependence of absorption coefficient with wavelength follows a power law, with the exponent as the Angstrom exponent. It is inversely dependent on the average size of particles in the aerosols.

$$\frac{\alpha_1}{\alpha_2} = \left(\frac{\lambda_1}{\lambda_2} \right)^{-\gamma} \quad (2.20)$$

The aethalometer has an inlet for the air, and contains a spool of filter, which automatically rotates to replace the sensing area with a fresh patch once a set number of particulates have been deposited. It is capable of finding the absorption coefficient at 7 discrete wavelengths; 370 nm, 470 nm, 520 nm, 590 nm, 660 nm, 880 nm, 950 nm. The Angstrom exponent can be found by fitting the absorption to a power law fit.

Chapter 3

Experimental Setup

The goal of the project is to demonstrate a method for highly sensitive, in-situ, real-time measurement of SSA of microplastic aerosols. The lab setup to test this involves passing microplastic aerosols through two IBBCEAS cavities in the 400 to 550 nm and 650 to 680 nm range, for a broad-spectrum analysis of the extinction coefficient ϵ , and the aethalometer to retrieve the absorption coefficient α . SSA can then be derived using the absorption and extinction coefficient.

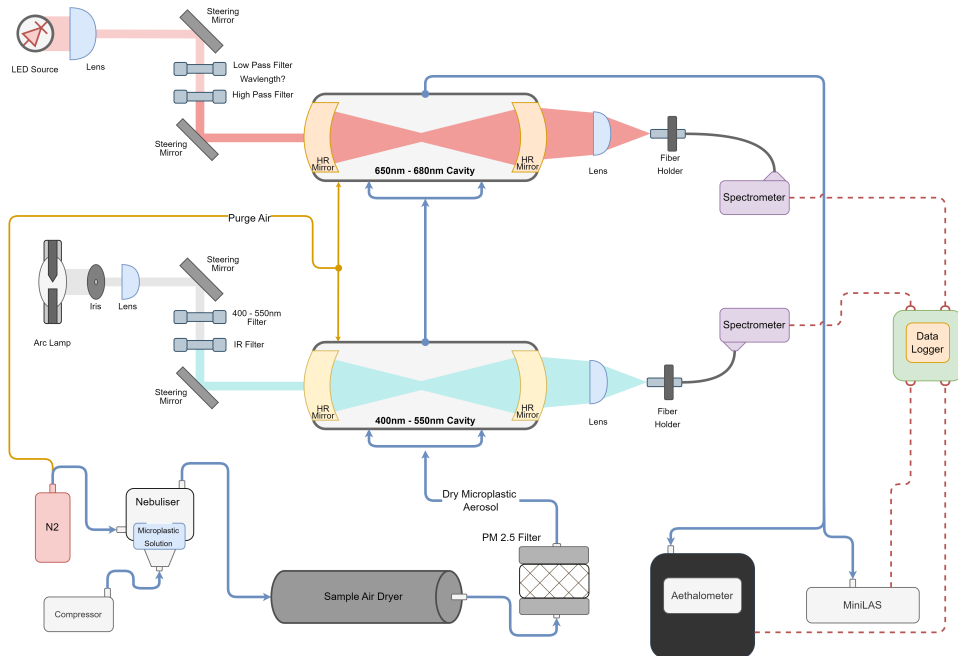


Figure 3.1: Schematic of the entire measurement setup

A nebuliser produces the aerosols from a solution of microplastics, which is then dried and filters out larger particles. This stream passes through the two IBBCEAS

cavities and then through the aethalometer. Three microplastics, Acrylonitrile butadiene styrene (ABS), polymethyl methacrylate (PMMA) and Polycaprolactone (PCL) were used for this experiment, as well as a NaCl aerosol for control. As inhalation of microplastic is potentially harmful, care was taken to ensure the gas stream under experimentation is not released into the atmosphere at any point.

Detailed explanations of the various components and methodology are given in the following sections.

3.1 Creating microplastic solution

The microplastic solutions were developed using good solvent bad solvent precipitation method[15]. A fixed mass of each plastic was slowly dissolved in Tetrahydrofuran (THF), which is a good solvent of all the three microplastics used (ABS, PCL, PMMA). Water, which is a bad solvent of plastic is then slowly added and mixed consistently. The dissolved plastics precipitate out as microplastics. The THF is then evaporated, leaving behind a suspension of microplastics.

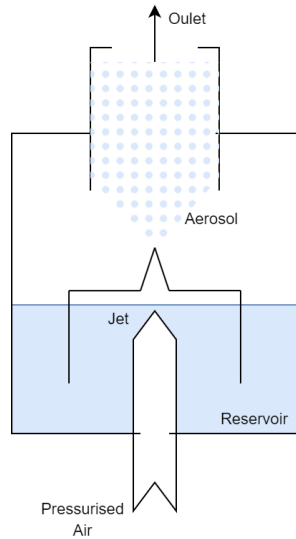
2 mg of each plastic in pure pellet form was dissolved in 10 ml of THF solution and stirred to dissolve completely. 20 ml of water was added slowly while stirring continuously. The solution was left under a fume hood for two days till the THF has safely evaporated.

3.2 Generation of aerosols

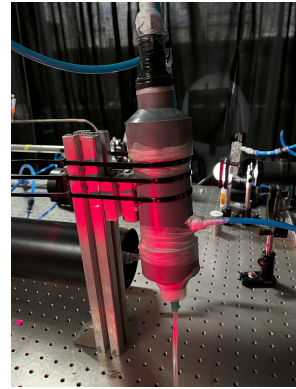
Commercial grade aerosol generators, which produce consistent and well-defined concentrations of a given particle are expensive. As Single Scattering Albedo is an intensive property, independent of concentration of particulate matter, an off the shelf, medical grade jet nebuliser was used to generate aerosols from the microplastic solution. Jet nebulisers pass compressed air through a narrow nozzle, creating a high-speed jet of air, and a vacuum in the wake. This vacuum pulls in the solution, atomising it and mixing it with the jet stream.

The nebuliser produces a mist, but did not have enough pressure to push the aerosol through the setup, so a system was made where the aerosol is uniformly mixed with

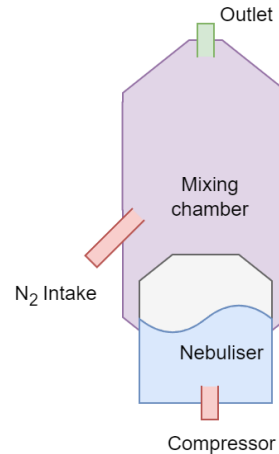
pressurised nitrogen at a steady flow rate to create a stream of aerosol with sufficient flow rate. The schematic and implementation of these systems are shown below.



(a) Schematic of nebuliser



(b) Mixing chamber



(c) Schematic of mixing chamber

The nitrogen intake nozzle is fixed at an angle to produce turbulence and facilitate mixing. This setup produces a steady stream of aerosol containing the microplastic, water vapour and nitrogen. The next step is drying the gas stream.

3.3 Sample Dryer

In order to remove humidity from the aerosol stream, a Sample Stream Dryer from Magee Scientific was used. It uses a proprietary NafionTM membrane-based permeation layer to remove water vapour from the stream without affecting any of the other constituents.

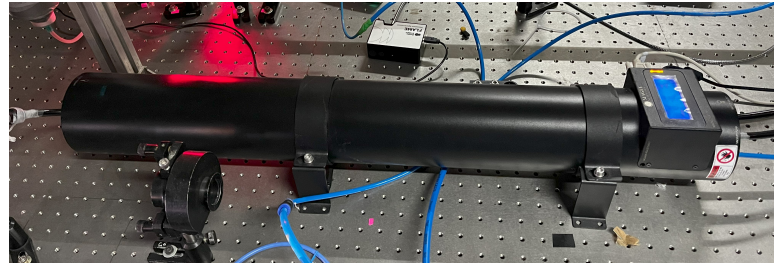
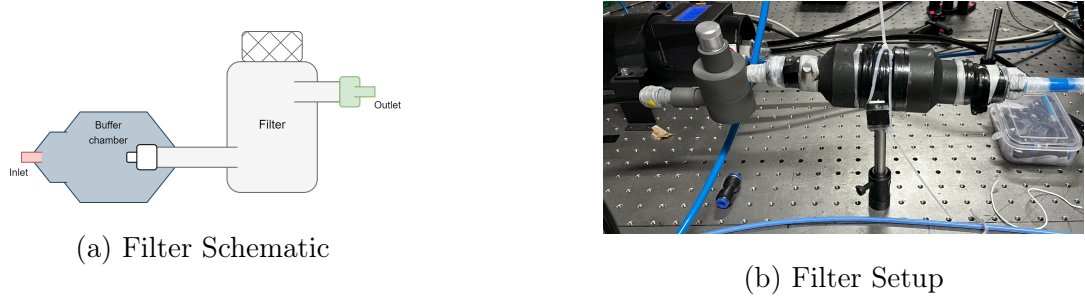


Figure 3.3: Magee Scientific sample air drier

3.4 $2.5\mu\text{m}$ filter

The medical grade nebuliser has no defined control over particle size. Aerosols over a certain size could have a large extinction value and could prove difficult to properly characterise with the IBBCEAS as most of the intensity could be attenuated, producing noisy, low intensity signal. A $2.5\mu\text{m}$ filter was used to filter out larger particles. It was built with filtering atmospheric air in mind so has no dedicated inlet, only an opening. To ensure the aerosols can enter without leaking into the atmosphere, a housing was made to enclose the inlet of the filter and the aerosol inlet.

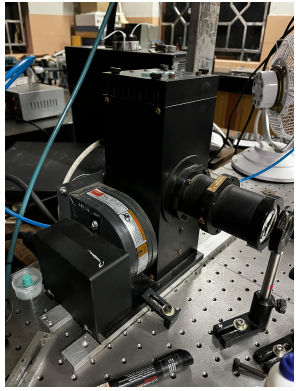


3.5 Light sources

The IBBCEAS cavity light source should have a broad, stable emission spectrum and a long-life time, with low spectral noise. The Arc Lamp and LED used in this setup matches the criteria for in-lab testing[4].

Xe Arc Lamp A Xe Arc discharge lamp was used to produce a broad spectrum high intensity light source for the 400 to 550 nm cavity.

Collimated High-Power LED Source A Thorlabs' M660L3-C2 660 nm LED was used for the 650 to 680 nm cavity.



(a) Arch Lamp



(b) High Power LED

3.6 400 to 550 nm Cavity

The cavity consists of two Altechna High Reflectivity (HR) 400 to 550 nm mirrors, with 99.98% reflectivity mounted on holders, two silver coated steering mirrors, a 400 to 550 nm bandpass filter, a Xe Arc Lamp and lenses for focusing. The light exiting the cavity is focused onto a fibre, which then passes onto an Ocean Optics HR4000 Spectrometer to log the cavity intensity counts. The cavity is enclosed with a 100 cm long stainless-steel chamber with inlets and outlets to pass the sample stream.

This cavity measures the extinction coefficient in the 400 to 550 nm range. Detailed explanations of the building and calibration will be covered in the next section.

3.7 650 to 680 nm Cavity

The 650 to 680 nm cavity is similar in operating principle to the 400 to 550 nm cavity. It uses Altechna HR mirrors in 620 m to 720 nm cavity with 99.9% reflectivity and a 660 nm High Power Collimating LED as light source. 650 nm high pass and 700 nm low pass filters are used to limit light outside the operating range.

The light exiting the cavity is focused onto a fibre and measured with an Ocean Optics Flame spectrometer.

3.8 Aethalometer

After passing through both cavities, the aerosol stream is passed through the aethalometer to measure the absorption coefficients. The microplastics are deposited onto the

aethalometer filter and the sample stream is safely released to the atmosphere.

3.9 Connections and Source

N₂ gas was mixed with the aerosol to improve flow rate. The cavities require a constant flow of clean air over the mirrors to avoid corrosion of film or contaminant deposition when test aerosols are passed in the cavity. A zero-air generator from Thermo Environment Instruments, which takes in atmospheric air and generates a dry, impurity free supply of air was sent through separate inlets near the mirror mounts. This intake has very low flow rate and the dilution of the aerosol stream due can be considered negligible[16].

The aerosols and the purge air are passed through pneumatic hoses and the various components were joined with pneumatic connectors. Every connection was tightly sealed with Parafilm to avoid leakage of the hazardous aerosols.

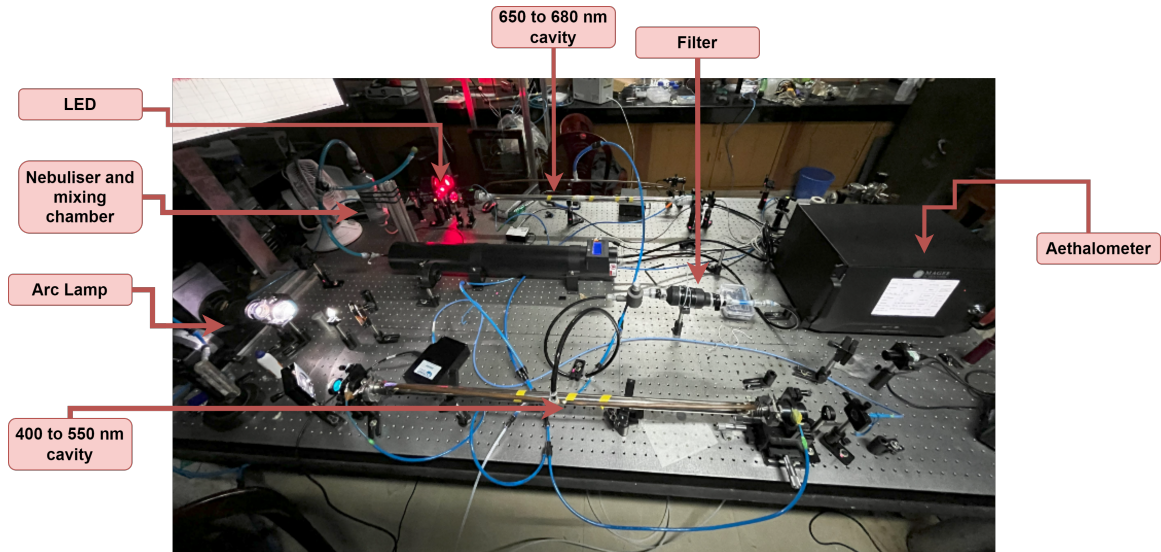


Figure 3.6: Lab setup

Chapter 4

Building and Calibrating the IBBCEAS Cavities

4.1 Cavity setup

4.1.1 Initial setup and laser alignment

The required parts are placed on the optical bench at their approximate locations. The HR mirror mounts are placed at a separation of 100 cm, with one of the mounts placed on a horizontal translation stage. The arc lamp and its steering mirrors are placed at the input end. A 550 nm Holmarc diode laser and steering mirrors are placed at the output end.

The laser steering mirrors are used to guide the laser beam through the mirror mounts. The laser and mirrors are aligned such that the beam is parallel to the optical bench surface. The beam height was set at 13.5 cm, corresponding to the height of the arch lamp. Pinholes are placed in the mounts, and the laser beam is aligned using the steering mirrors such that it passes through both pinhole centres, while staying parallel to the bench surface. This ensures the HR mirrors will be at the same height.

4.1.2 Arc lamp alignment

The arc lamp light is steered into the cavity. The focusing lens for the arc lamp are placed in front of the arc lamp such that the image of the arc source focuses at the

centre of the cavity, after passing through the steering mirrors. The steering mirrors are used to guide the arc lamp light such that the centre of the arc image coincides with the laser beam at both ends of the cavity. An aperture is used to reduce the intensity of the light to help see the image better. After alignment, the laser beam should hit the centre of the arc lamp. This ensures that the arc lamp light passes through the centre of the HR mirrors, and is parallel to the bench.

4.1.3 HR mirror alignment

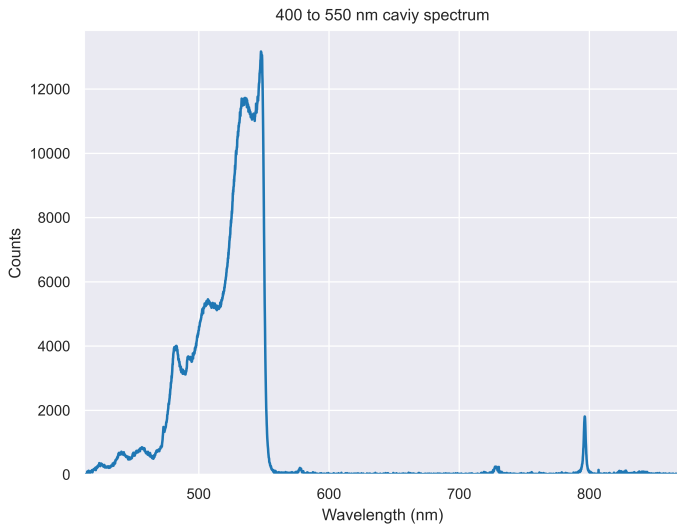
The first HR mirror is placed at the input end, making sure the concave side faces inwards, and secured tightly with flange mounts and O-ring to prevent leakage. The thumb screws on the mount were adjusted such that the laser beam hitting the mirror retraces its path. The second mirror is placed and also aligned to ensure the laser beam retraces its path. Lastly, fine adjustments should be made to confirm that only one beam spot is visible on both the mirrors.

4.1.4 Output light collection

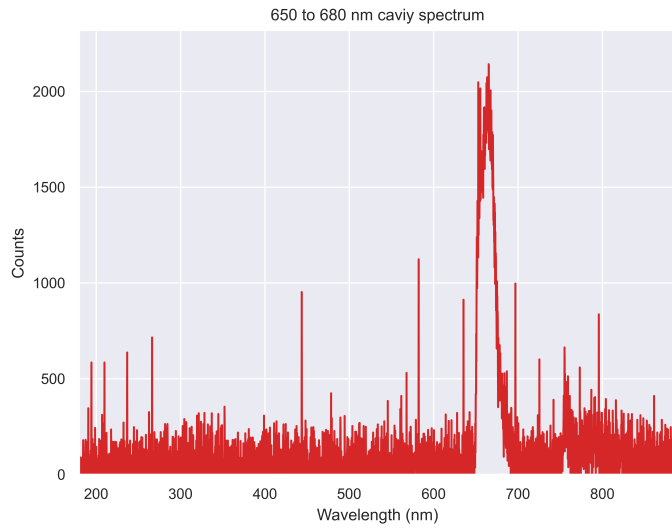
The arc lamp is turned on, and a short focal length lens is placed at the output end and the light from the arc lamp is focused to a point. An optical fiber mounted on a holder is placed at this point. The bandpass filter is placed after the arc lamp, and the fiber is connected to the spectrometer. Care must be taken to always place the filter before connecting the spectrometer as the high intensity light could damage the instrument.

4.1.5 Verification and optimization

High intensity counts should be visible in the 400 to 550 nm range. It can be verified that the signal is indeed a cavity signal by slightly misaligning one of the mirrors and noting the sharp drop in intensity. Fine adjustments are made to the mirrors till the count is optimized.



(a) 400 to 550 nm cavity spectrum



(b) 600 to 680 nm cavity spectrum

4.1.6 Chamber mounting

The translation stage is used to move the mirrors apart, and the chamber is placed in between and tightened. O-rings and clamps are used to ensure tight seal. Fine adjustments are made to ensure the cavity is aligned and the signal count is high.

4.2 Cavity Calibration

Calculating the reflectivity of the cavity is an essential step to finding the absorption.

Nitrogen dioxide (NO_2) based calibration was used to find reflectivity of both the 400 to 550 nm cavity and 650 to 680 nm cavity[17]. Cavity intensity fluctuations for known concentrations of NO_2 and N_2 were compared and known absorption cross-sections were taken from the MPI-Mainz UV/VIS Spectral Atlas of Gaseous Molecules of Atmospheric Interest[18] database and reflectivity calculated for wavelengths in the 400 to 550 nm range.

At STP, given NO_2 concentration = 9.1 ppm:

$$n = (9.1 \times 10^{-6}) \cdot (2.45 \times 10^{19}) = 2.23 \times 10^{14} \text{ particles/cm}^3 \quad (4.1)$$

extinction coefficient ϵ :

$$\epsilon = n * \sigma_{ext} = \left(\frac{I_O}{I} - 1 \right) \frac{(1 - R)}{d} \quad (4.2)$$

$$R = 1 - \frac{n\sigma_{abs}d}{\frac{I_O}{I} - 1} \quad (4.3)$$

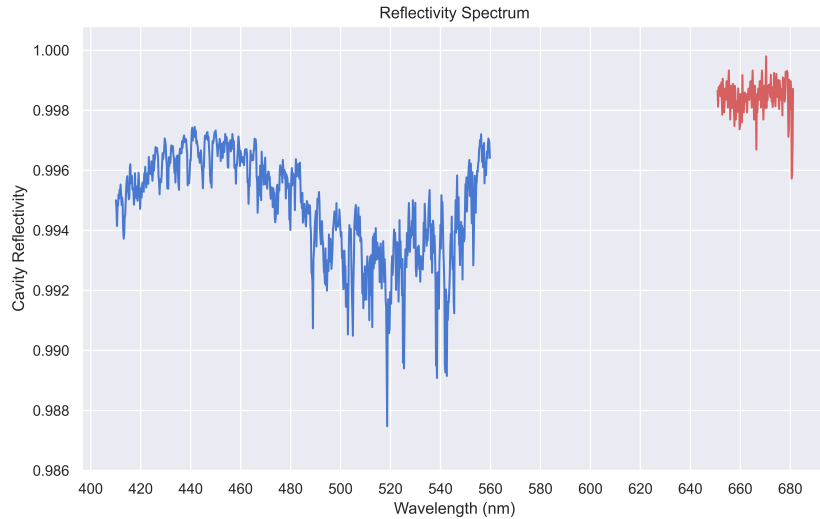


Figure 4.2: Reflectivity spectrum of both cavities

Chapter 5

Experiments and data collection:

5.1 Data collection

The aerosols for PCL, PMMA, ABS and NaCl were generated and passed through both cavities and the data was collected for each sample. The spectrometers were connected to the OceanView app and the spectrum data was collected for every update interval. The aethalometer automatically logs data.

Each aerosol was passed through the cavities and aethalometer for a duration of 5 minutes, during which there was a notable decrease in intensity in the cavity and an increase in aethalometer count. After each sample, the nebuliser was thoroughly cleaned with DI water and the readings were allowed to return to normal and stabilise before passing the next aerosol.



Figure 5.1: Data collected from the various instruments

5.2 Data analysis and results

The cavity spectrometers output the data files containing intensity counts for each wavelength. The aethalometer outputs data as a single file with various sensor outputs in time, from which Black Carbon (BC) values were extracted.

Python scripts were written to parse and compile the collected data from the various instruments and generate Pandas DataFrame Objects for easy and efficient access. The timebases and wavelengths of each instrument was different, so the data points were interpolated in both axes to a common timebase, with an interval of 1s and a common wavelength, equal to the wavelength domains of both spectrometers

The data was averaged over the time interval each aerosol was passed to obtain the mean value for the corresponding aerosols.

The aethalometer data consisted of black carbon concentration values at each of the discrete wavelengths. This can be converted to absorption coefficient using the formula

$$\alpha(\lambda) = \sigma_{abs}(\lambda) * BC_\lambda \quad (5.1)$$

The observed and calculated data can be interpolated over the entire spectrum to obtain absorption coefficient spectra of each aerosol. The data was also used to find the Angstrom coefficient of each aerosol.

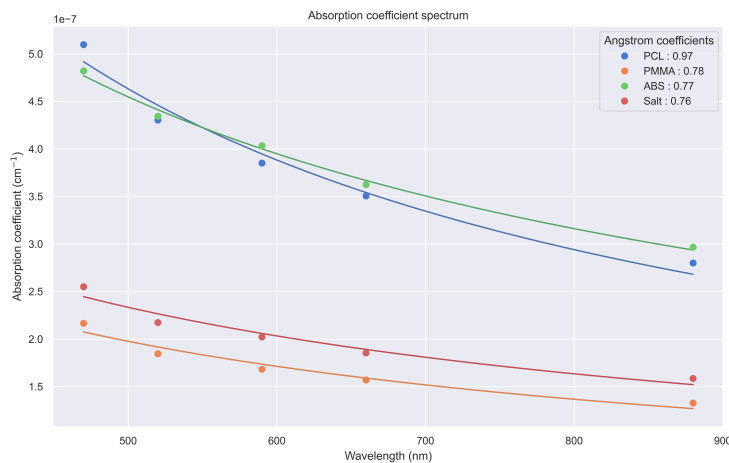


Figure 5.2: Absorption coefficient with power law fitting

The spectrometer output, combined with the interpolated reflectivity spectrum was

used to find extinction coefficient spectrum of each aerosol using the formula:

$$\epsilon = \left(\frac{I_O}{I} - 1 \right) \frac{(R - 1)}{d} \quad (5.2)$$

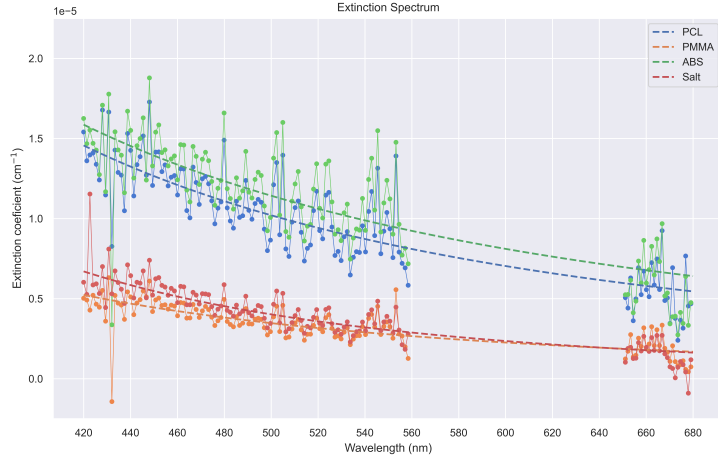


Figure 5.3: Extinction spectrum, with power law fitting

The absorption and extinction coefficient values are used to find the single scattering albedo according to the formula

$$SSA = \frac{\epsilon - \alpha}{\epsilon} \quad (5.3)$$

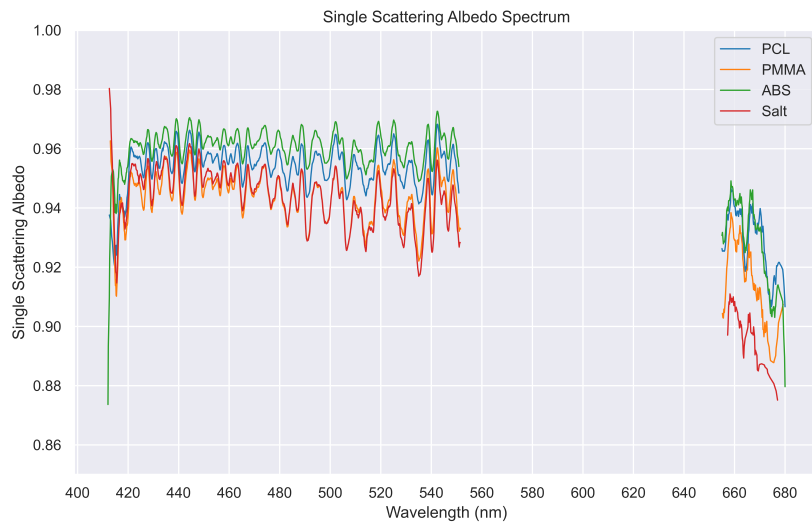


Figure 5.4: Single Scattering Albedo

Chapter 6

Discussions and outlook

Throughout this experimental study, the extinction and absorption coefficient of various microplastic aerosols were calculated, and the SSA was determined. The single scattering albedos were found to be in the 0.8-0.9 range, in agreement with computer models[2]. The aerosol microplastics are predominantly scattering microplastics with high SSA. This means that an increase in microplastic concentration in the atmosphere could lead to potential cooling of the Earth's surface

The experiment proved the feasibility of implementing a highly sensitive and robust in-situ monitoring of microplastic SSA measurements. Future work in the field could use electrostatic separators and filters to separate and remove carbonaceous aerosols, and measure the SSA of microplastics in the region, giving us real-time insights into the radiative forcing effects of microplastics.

In future research, particle size analysers can be added to the setup to calculate the complex refractive index of microplastics using Inverse Mie calculations[19]. This enables identification and characterisation of the various types of microplastics. The pellets used to prepare the microplastic aerosols were colourless or white. In the real world microplastic pollution is more likely to be coloured could have lower SSA values than the white microplastics used in this experiment. Measurements can be made with such coloured microplastic aerosols to study how dyes affect the radiative forcing effects. More cavities can be added to cover a larger portion of the Sun's spectrum.

In summary, a combination of IBBCEAS and Aethalometer was used to demonstrate a method of highly sensitive, real-time in situ measurements of SSA of various microplastic aerosols, to aid research into the climatic effects of microplastics.

Bibliography

- [1] Hannah Ritchie, Veronika Samborska, and Max Roser. “Plastic Pollution”. In: *Our World in Data* (Dec. 28, 2023). [Online; accessed 2024-04-25]. URL: <https://ourworldindata.org/plastic-pollution>.
- [2] Laura E. Revell et al. “Direct radiative effects of airborne microplastics”. en. In: *Nature* 598.7881 (Oct. 2021), pp. 462–467. ISSN: 0028-0836, 1476-4687. DOI: 10.1038/s41586-021-03864-x.
- [3] Zike Huang, Bo Hu, and Hui Wang. “Analytical methods for microplastics in the environment: a review”. en. In: *Environmental Chemistry Letters* 21.1 (Feb. 2023), pp. 383–401. ISSN: 1610-3653, 1610-3661. DOI: 10.1007/s10311-022-01525-7.
- [4] Aiswarya Saseendran et al. “Dual-cavity spectrometer for monitoring broadband light extinction by atmospheric aerosols”. en. In: *Aerosol Science and Technology* 54.10 (Oct. 2020), pp. 1183–1196. ISSN: 0278-6826, 1521-7388. DOI: 10.1080/02786826.2020.1763249.
- [5] National Oceanic and Atmospheric Administration US Department of Commerce. *What are microplastics?* EN-US. URL: <https://oceanservice.noaa.gov/facts/microplastics.html> (visited on 04/30/2024).
- [6] Ahmed I. Osman et al. “Microplastic sources, formation, toxicity and remediation: a review.” eng. In: *Environmental chemistry letters* (Apr. 4, 2023). publisher-place: United States PMID: 37362012 PMCID: PMC10072287, pp. 1–41. ISSN: 1610-3653 1610-3661. DOI: 10.1007/s10311-023-01593-3.
- [7] Krzysztof Bohdan and Kevin C. Honeychurch. “Under-researched and under-reported new findings in microplastic field”. en. In: *Science of The Total Environment*

ment 918 (Mar. 2024), p. 170466. ISSN: 00489697. DOI: 10.1016/j.scitotenv.2024.170466.

- [8] Albert A. Koelmans et al. “Microplastics in freshwaters and drinking water: Critical review and assessment of data quality”. en. In: *Water Research* 155 (May 2019), pp. 410–422. ISSN: 00431354. DOI: 10.1016/j.watres.2019.02.054.
- [9] Kui Li et al. “Microplastic pollution as an environmental risk exacerbating the greenhouse effect and climate change: a review”. en. In: *Carbon Research* 3.1 (Jan. 2024), p. 9. ISSN: 2731-6696. DOI: 10.1007/s44246-023-00097-7.
- [10] 2.4: *Surfaces - Single-scattering Albedo*. en. [Online; accessed 2024-04-24]. Jan. 25, 2017. URL: [https://phys.libretexts.org/Bookshelves/Astronomy_-Cosmology/Planetary_Photometry_\(Tatum_and_Fairbairn\)/02%3A_Albedo/2.04%3A_Surfaces_-_Single-scattering_Albedo](https://phys.libretexts.org/Bookshelves/Astronomy_-Cosmology/Planetary_Photometry_(Tatum_and_Fairbairn)/02%3A_Albedo/2.04%3A_Surfaces_-_Single-scattering_Albedo).
- [11] Lu Zhang et al. “Clear-Sky Direct Aerosol Radiative Forcing Uncertainty Associated with Aerosol Optical Properties Based on CMIP6 models”. In: *Journal of Climate* 35.10 (May 2022), pp. 3007–3019. ISSN: 0894-8755, 1520-0442. DOI: 10.1175/JCLI-D-21-0479.1. URL: <https://journals.ametsoc.org/view/journals/clim/35/10/JCLI-D-21-0479.1.xml> (visited on 04/28/2024).
- [12] Aiswarya S. “Optical properties of atmospherically relevant aerosols instrumentation measurements and retrieval”. English. In: *University* (2021). URL: <https://shodhganga.inflibnet.ac.in:8443/jspui/handle/10603/434584> (visited on 04/30/2024).
- [13] Kaiyuan Zheng et al. “Review of Incoherent Broadband Cavity-Enhanced Absorption Spectroscopy (IBBCEAS) for Gas Sensing”. en. In: *Sensors* 18.11 (Oct. 2018), p. 3646. ISSN: 1424-8220. DOI: 10.3390/s18113646.
- [14] E. Weingartner et al. “Absorption of light by soot particles: determination of the absorption coefficient by means of aethalometers”. en. In: *Journal of Aerosol Science* 34.10 (Oct. 2003), pp. 1445–1463. ISSN: 00218502. DOI: 10.1016/S0021-8502(03)00359-8.
- [15] Athiyanathil Sujith et al. “Natural dye-doped poly(methyl methacrylate) microparticles for nonlinear optics”. en. In: *Micro & Nano Letters* 9.9 (Sept. 2014), pp. 566–568. ISSN: 1750-0443, 1750-0443. DOI: 10.1049/mnl.2013.0754.

- [16] Shebin John et al. “A broadband cavity-enhanced spectrometer for atmospheric aerosol light extinction measurements”. en. In: *Aerosol Science and Technology* 55.11 (Nov. 2021), pp. 1264–1276. ISSN: 0278-6826, 1521-7388. DOI: 10.1080/02786826.2021.1944604.
- [17] liu-yi Ling et al. “Calibration Method of Broadband Cavity Enhanced Absorption Spectroscopy for Measuring Atmospheric NO₂”. In: *Guang Pu Xue Yu Guang Pu Fen Xi/Spectroscopy and Spectral Analysis* 38 (Mar. 1, 2018), pp. 670–675. DOI: 10.3964/j.issn.1000-0593(2018)03-0670-06.
- [18] H. Keller-Rudek et al. “The MPI-Mainz UV/VIS Spectral Atlas of Gaseous Molecules of Atmospheric Interest”. en. In: *Earth System Science Data* 5.2 (Dec. 2013), pp. 365–373. ISSN: 1866-3516. DOI: 10.5194/essd-5-365-2013. URL: <https://essd.copernicus.org/articles/5/365/2013/> (visited on 04/26/2024).
- [19] Aiswarya Saseendran et al. “Retrieval of Broadband Optical Properties from Ambient Aerosols Measurements Using Inverse Mie Calculations”. en. In: *Aerosol Science and Engineering* 6.1 (Mar. 2022), pp. 111–125. ISSN: 2510-375X, 2510-3768. DOI: 10.1007/s41810-021-00128-z.